Reactive Scattering of OD Radicals with ICl and Br_2 Molecules at Initial Translational Energy $E \sim 90$ kJ mol^{-1}

S. Mohr, K. M. Goonan, D. D. Wells, and R. Grice*

Chemistry Department, University of Manchester, Manchester, M13 9PL, U.K.

Received: July 10, 1997; In Final Form: October 2, 1997[⊗]

Reactive scattering of OD radicals with ICl and Br_2 molecules has been studied at an initial translational energy $E \sim 90$ kJ mol^{-1} using a supersonic beam of OD radicals seeded in He buffer gas generated from a high-temperature radio frequency discharge source. The center-of-mass angular distribution of DOI scattering from OD + ICl shows sharp forward and backward peaking with the relative intensity of the backward peak being lower by a factor $\sim 0.6 \pm 0.1$. The DOBr scattering from OD + Br_2 shows broader peaking in the forward direction declining to a lower intensity $\sim 0.8 \pm 0.2$ in the backward direction. In both cases the product translational energy distributions peak at low energy with a tail extending out to higher energy. Comparison with the predictions of phase space theory indicates that the OD + ICl reaction proceeds via a DOICl collision complex with a lifetime of approximately one rotational period, while the OD + Br_2 reaction shows evidence for the migration of the OD radical between the Br atoms of a DOBrBr complex. The DOICl complex corresponds to a significant well of depth $E_0 \sim 80$ kJ mol^{-1} on the potential energy surface for the OD + ICl reaction while the potential energy surface for the OD + Br_2 reaction also supports a shallow minimum.

Introduction

The first molecular beam study[1] of OH radicals reacting with Br_2 molecules employed an effusive free-radical source in which NO_2 molecules were injected into a flow of H atoms in excess H_2 molecules arising from a low-pressure microwave discharge source. More recently, a supersonic beam of OH radicals seeded in He buffer gas generated from a high-pressure radio frequency discharge of H_2O/He mixture has been used to study their hydrogen atom displacement reactions[2,3] with CO and D_2 molecules. Accordingly, a high-pressure radio frequency discharge of D_2O/He mixture in a high-temperature ceramic source which was previously employed to produce a high-energy O atom beam[4] has been used to produce a supersonic beam of OD radicals seeded in He buffer gas which also includes both O and D atoms. This high-temperature radio frequency discharge source has been used to study the reactive scattering of OD radicals with ICl and Br_2 molecules at high initial translational energies $E \sim 90$ kJ mol^{-1}.

$$\mathrm{OD} + \mathrm{ICl} \rightarrow \mathrm{DOI} + \mathrm{Cl} \quad (1)$$

$$\mathrm{OD} + \mathrm{Br_2} \rightarrow \mathrm{DOBr} + \mathrm{Br} \quad (2)$$

A room-temperature rate constant $k \sim 2.6 \times 10^{10}$ dm^3 mol^{-1} s^{-1} has been determined for reaction 2 by discharge flow resonance fluorescence measurements.[5,6] Measurements at atmospheric pressure[7,8] for the analogous reaction of I_2 molecules yield a rate constant $k \sim 1.1 \times 10^{11}$ dm^3 mol^{-1} s^{-1} but the OH + ICl reaction[8] under these conditions yields HOCl rather than HOI as the predominant reaction product.

Experimental Section

The apparatus was the same as that employed[9,10] to study the reactive scattering of O atoms with ICl and Br_2 molecules at high initial translational energies. The radio frequency discharge source[11] employed a vapor pressure ~9 mbar of D_2O in a pressure ~140 mbar of He buffer gas maintained by bubbling He gas through liquid D_2O in a reservoir at a temperature ~6 °C just above the freezing point. The velocity distribution of the OD radical beam was measured by a beam monitor mass spectrometer to gain the peak velocity v_{pk}, full width at half-maximum intensity v_{wd} and Mach number quoted in Table 1. The ICl and Br_2 molecules were both seeded in N_2 buffer gas expanded from a monel nozzle of diameter ~0.1 mm. Vapor pressures ~25 mbar for ICl and ~120 mbar for Br_2 were maintained by a reservoir at ~15 °C with a flow of N_2 buffer gas at pressures ~100 and ~500 mbar. The ICl and Br_2 beam velocity distributions were measured by pseudorandom cross correlation time-of-flight analysis[12] using the rotatable mass spectrometer detector to gain the velocity parameters quoted in Table 1.

TABLE 1: Beam Velocity Distributions: Peak Velocity v_{pk}, Full Width at Half-Maximum Intensity v_{wd} and Mach Number *M*

beam	v_{pk}/m s^{-1}	v_{wd}/m s^{-1}	*M*
OD (He)	3300	1000	6
ICl (N_2)	530	145	7
Br_2 (N_2)	750	185	8

Results

Angular distribution measurements of DOI and DOBr reactive scattering yield ~30 and ~5 counts s^{-1} against backgrounds ~100 and ~30 counts s^{-1} at the 145 and 99 mass peaks, respectively. The reactive scattering signal was measured as a modulated difference in those channels at short times which contribute to scattered DOI and DOBr products in order to discriminate against backgrounds arising from ambient molecules at low velocities. The laboratory angular distribution of DOI scattering in Figure 1 is located close to the laboratory centroid but the DOBr scattering in Figure 2 extends over a slightly wider angular range. The laboratory velocity distributions of DOI scattering in Figure 3 and DOBr scattering in Figure 4 were obtained using repeated integration times

[⊗] Abstract published in *Advance ACS Abstracts,* November 15, 1997.

S1089-5639(97)02236-6 CCC: $14.00

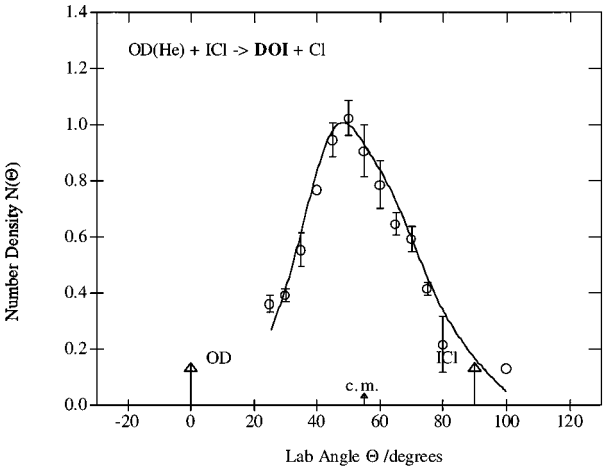

Figure 1. Laboratory angular distribution (number density) of DOI reactive scattering from OD + ICl at initial translational energy $E \sim$ 94 kJ mol^{-1}. Solid line shows the fit of the kinematic analysis.

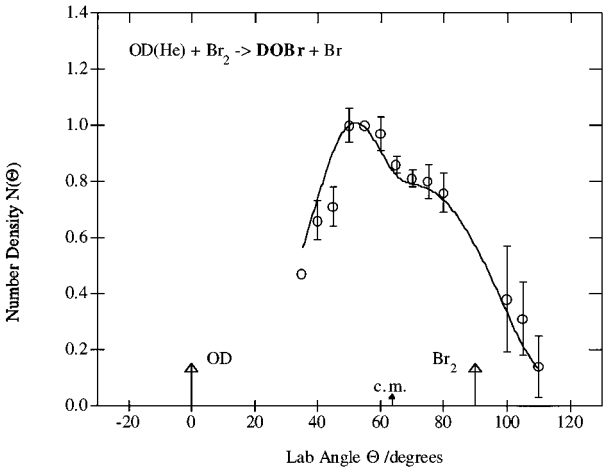

Figure 2. Laboratory angular distribution (number density) of DOBr reactive scattering from OD + Br_2 at initial translational energy $E \sim$ 88 kJ mol^{-1}.

~2000 s to gain signal-to-noise ratios ~10 at the peaks of the distributions. Kinematic analysis of these data employed the forward convolution method[13] with the differential cross section expressed as a product of an angular function $T(\theta)$ and a velocity function $U(u)$

$$I_{cm}(\theta,u) = T(\theta)\, U(u) \qquad (3)$$

The angular distribution for DOI product in Figure 5 shows sharp forward and backward peaking with the intensity of the backward peak being lower by a factor ~0.6. The angular distribution for DOBr product in Figure 6 shows broader peaking in the forward direction which declines to a relative intensity ~0.7 in the backward direction. Both product translational energy distributions peak at low energy with a tail extending out to higher energy. The backward scattering has slightly higher peak product translational energy than the forward scattering for OD + Br_2. However, an acceptable fit to the OD + Br_2 laboratory data is also obtained when the intensity of backward peaking is increased to that of the forward peak and the product translational energy is independent of scattering angle. The peak E'_{pk} and average E'_{av} product translational energies are listed in Table 2 together with the initial translational energies E and reaction exoergicities ΔD_0 estimated from the DOI and DOBr bond energies of Rusic and Berkowitz[14] and the ICl and Br_2 bond energies of Huber and Herzberg.[15]

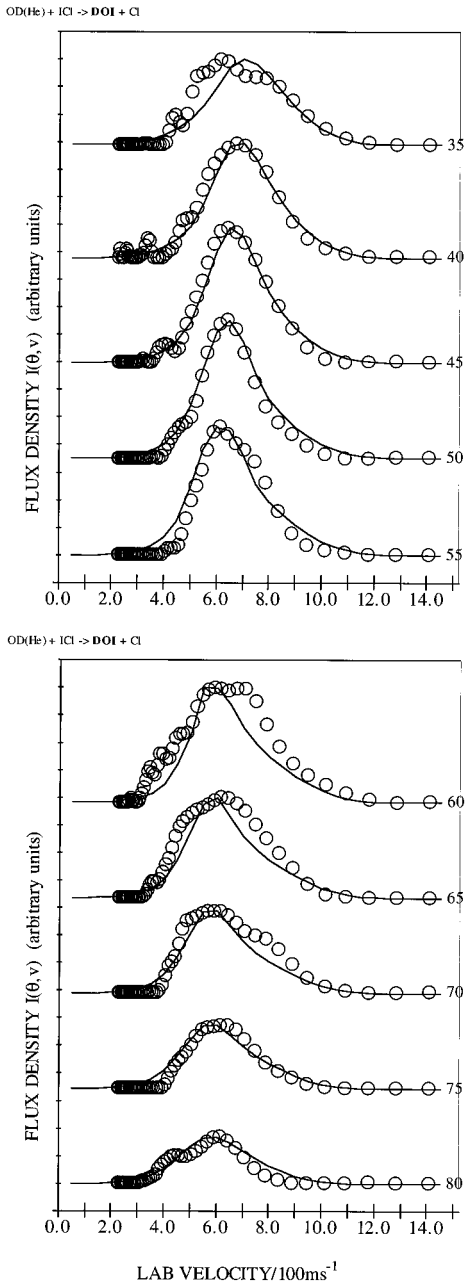

Figure 3. Laboratory velocity distributions (flux density) of reactively scattered DOI from OD + ICl at an initial translational energy $E \sim$ 94 kJ mol^{-1}. Solid line shows fit of the kinematic analysis.

No DOCl product was observed from the reaction of OD with ICl in these experiments.

Discussion

Previous measurements[1] of the OH + Br_2 reaction at very low initial translational energy have shown evidence for reaction via a long-lived HOBrBr complex for which a bent staggered configuration was proposed. While the depth of the potential energy well corresponding to this complex must be significantly greater than the reaction exoergicity, its stability is not further defined by these early experimental data. The center of mass angular distribution of DOI reaction product in Figure 5 is indicative of reaction via a DOICl collision complex with a lifetime[16] approximately equal to its rotational period. Phase space theory[17−19] predicts the product translational energy distribution arising from the dissociation of such a persistent complex when this is unimpeded by any potential energy barrier

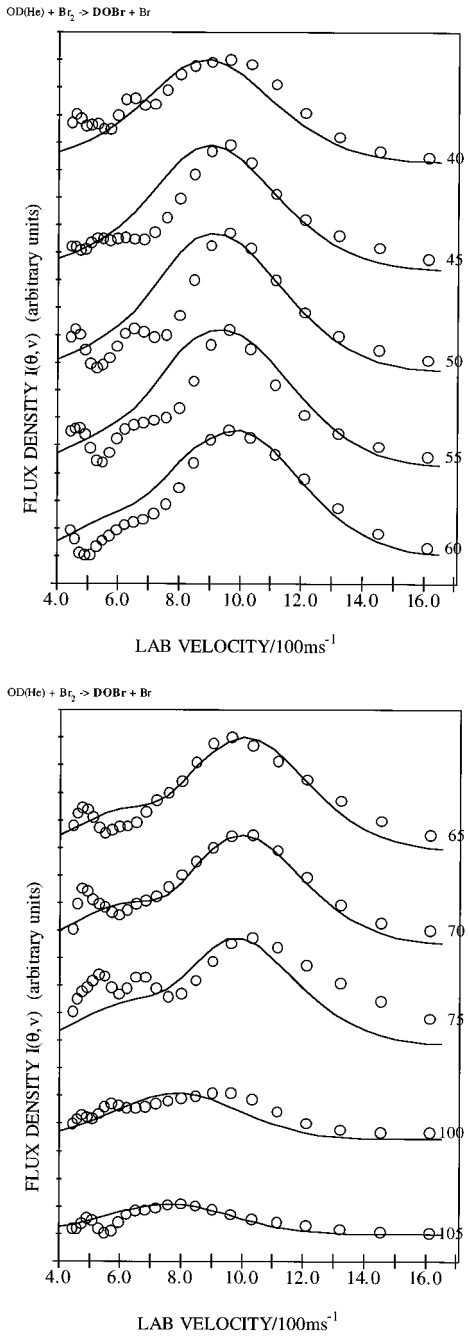

Figure 4. Laboratory velocity distributions (flux density) of reactively scattered DOBr from OD + Br_2 at initial translational energy $E \sim 88$ kJ mol^{-1}.

in the exit valley of the potential energy surface. The prediction in Figure 7 calculated with initial $b_m = 2.0$ Å and final $b'_m = 5$ Å maximum impact parameters using the DOI vibrational frequencies of Walker et al.[20,21] shows good agreement with the experimental product translational energy distribution. The angular distribution of DOI scattering may be calculated by the extended phase space model[22] in the form of a linear combination of angular functions

$$I(\theta) = c_0 + {}^1/_2 c_2 I(s = 3/2, a^2 = 1, \cos\gamma, \theta) + {}^3/_8 c_4 I(s = 5/2, a^2, \cos\gamma, \theta) \quad (4)$$

The coefficients c_0, c_2, c_4 and the parameter a^2 listed in Table 3 were determined by fitting to the distribution of the cosine of the helicity angle α lying between the initial **L** and final **L′** orbital angular momenta predicted by phase space

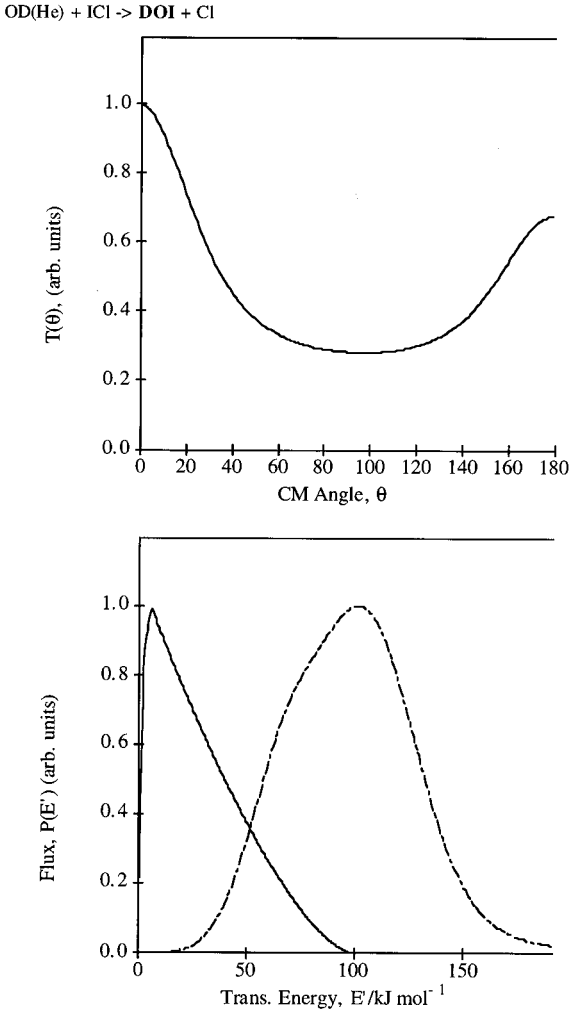

Figure 5. Angular function $T(\theta)$ and translational energy distribution $P(E')$ for DOI products from OD + ICl at initial translational energy $E \sim 94$ kJ mol^{-1}. Dashed energy curve shows the distribution of initial translational energy.

theory. Comparison of the experimental angular distribution and the prediction of eq 4 multiplied by the decay[16] function $\exp(-\theta/\theta^*)$ are in good agreement in Figure 7 when the value $\theta^* = 360°$ is employed. The parameter $\cos\gamma = J_{mp}/L_m$ represents the effect of ICl rotational angular momentum, where the most probable value $J_{mp} \sim 20\hbar$ compared with the maximum initial orbital angular momentum $L_m \sim 170\hbar$ yields a ratio $\cos\gamma \sim 0.1$.

This good agreement between the predictions of phase space theory and the observed DOI reactive scattering confirms the conclusion that the OD + ICl reaction proceeds via a persistent DOICl complex. However, the more broadly peaked forward scattering of DOBr product suggests that the OD + Br_2 reaction proceeds via a stripping mechanism with the DOBrBr intermediate persisting for only a fraction of a rotational period. This is in line with the trend[23] in the stability of halogen containing free-radical intermediates, which depends on the identity of the central halogen atom and is greater for the more electropositive I atom of DOICl than the Br atom of DOBrBr. Enhanced stability is attributed[24] to charge-transfer interaction of the form DO^-ICl^+ and to the lower exoergicity of the OD + ICl reaction. The lack of any observed DOCl product scattering in these experiments confirms the stability of the DOICl configuration. However, the observation of HOCl product in the kinetics experiments[8] at atmospheric pressure suggests that slow conversion to the DOClI configuration gives access to this exoergic

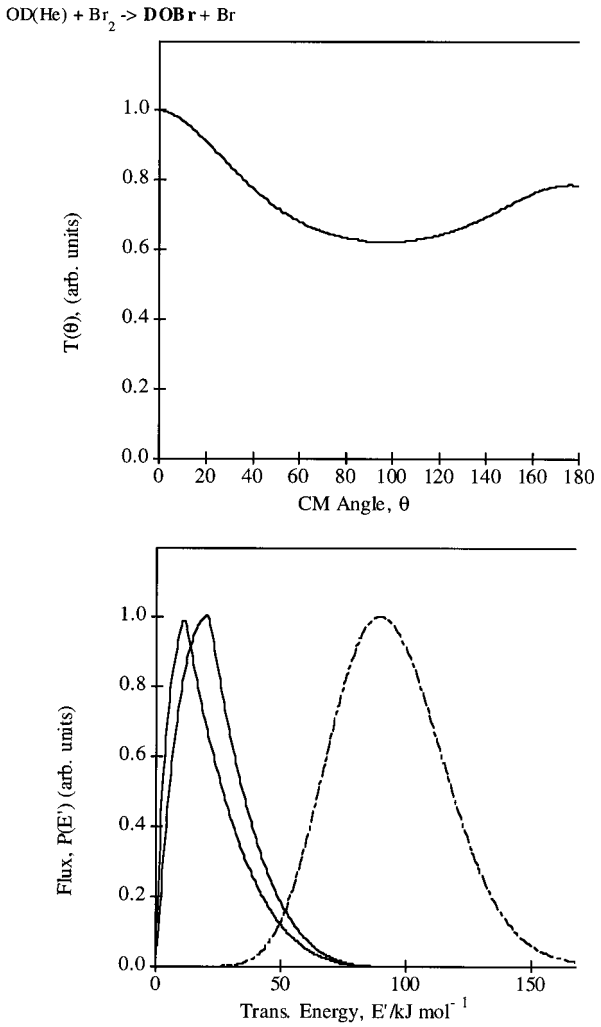

Figure 6. Angular function $T(\theta)$ and translational energy distribution $P(E')$ for DOBr products from OD + Br_2 at initial translational energy $E \sim 88$ kJ mol^{-1}. Left-hand product translational energy distribution denotes forward scattering, right-hand backward scattering.

TABLE 2: Reaction Energetics: Initial Translational Energy *E*, Peak Product Translational Energy E'_{pk}, Average Product Translational Energy E'_{av}, and Reaction Exoergicity ΔD_0

reaction	E/kJ mol^{-1}	E'_{pk}/kJ mol^{-1}	E'_{av}/kJ mol^{-1}	ΔD_0/kJ mol^{-1}
OD + ICl	94	5	29	-8 ± 12
OD + Br_2	88	11	21	13 ± 2

pathway. Similarly the observation of DOI product indicates that access to the alternative reaction pathway

$$\mathrm{OD + ICl \rightarrow DOICl \rightarrow OI + DCl} \qquad (5)$$

via a four-membered ring transition state is impeded by a potential energy barrier. The H−OI bond energy of Rusic and Berkowitz[14] suggests that while the rearrangement pathway of eq 5 may be exoergic $\Delta D_0 \sim 20 \pm 12$ kJ mol^{-1}, the corresponding rearrangement pathway for OD + Br_2 is endoergic $\Delta D_0 \sim -20 \pm 5$ kJ mol^{-1}.

The ratio of the lifetime τ to the rotational period τ_{rot} for the DOICl complex may be estimated from the RRKM formula[25]

$$\frac{\tau}{\tau_{rot}} \cong \frac{L_m}{4\Pi I_2^* \nu}\left(\frac{E + \Delta D_0 + E_0}{E + \Delta D_0}\right)^{s-1} \qquad (6)$$

This yields $\tau \sim \tau_{rot}$ when using a maximum initial orbital angular momentum $L_m \sim 170\hbar$, a moment of inertia $I^*_2 \sim 4 \times 10^{-45}$ kg m^2, a mean vibrational frequency $\nu = 1.1 \times 10^{13}$ s^{-1}, and an effective number of modes $s = 6$, when the well depth of the DOICl complex is taken as $E_0 \sim 80 \pm 20$ kJ mol^{-1}. This calculation assumes that the DOICl complex dissociates with roughly equal probability to form reaction products and to reform the reactants.

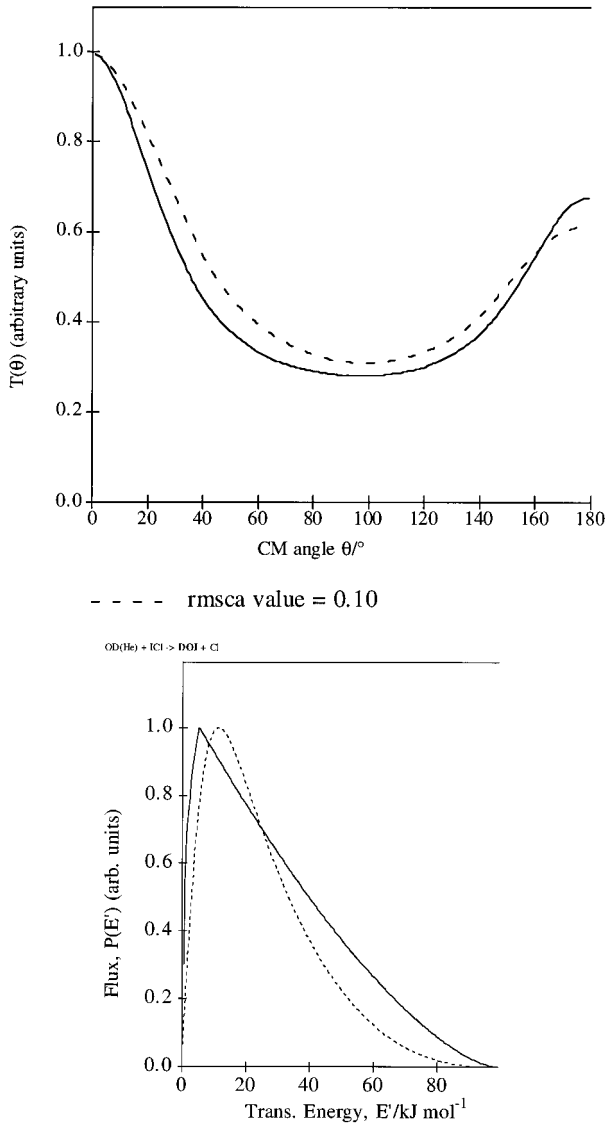

Figure 7. Angular distribution and product translational energy distribution for DOI scattering calculated from extended phase space theory (broken curves) compared with the experimental distributions (solid curves).

TABLE 3: Parameters for Extended Phase Space Theory: Maximum Initial b_m and Final b'_m Impact Parameters, Fitting Parameters c_0, c_2, c_4, and a^2 and Reactant Angular Momentum Parameter cos γ

b_m/Å	b'_m/Å	c_0	c_2	c_4	a^2	cos γ
2.0	5.0	0.03	0.17	0.59	1.84	0.1

The product translational energy distributions for the OD + Br_2 reaction in Figure 8 also show good agreement with the predictions of phase space theory. However, the angular distribution of DOBr scattering in Figure 4 is much broader than that predicted by phase space theory. This suggests the emergence of stripping dynamics with the OD radical migrating between the Br atoms of the DOBrBr complex. Hence the angular distribution for the OD + Br_2 reaction may reflect a collision lifetime which is now less than the rotational period

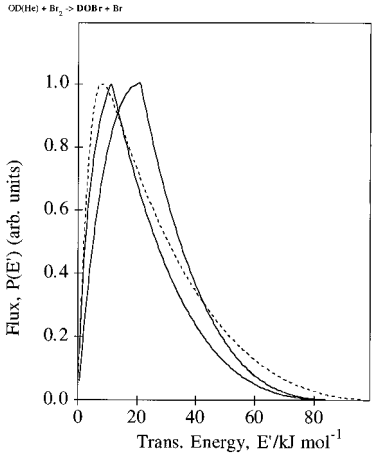

Figure 8. Product translational energy distribution for DOBr scattering calculated from phase space theory (broken curve) compared with the experimental distributions (solid curves). The experimental distributions reflect the range of uncertainty for the product translational energy of the backward scattering.

of the DOBrBr complex. The observation of stripping dynamics at high initial translational energy and a long-lived complex[1] at very low initial translational energy suggests the presence of a shallow well on this potential energy surface.

Acknowledgment. Support of this work by Engineering and Physical Sciences Research Council and the European Commission is gratefully acknowledged.

References and Notes

(1) Veltman, I.; Durkin, A.; Smith, D. J.; Grice, R. *Mol. Phys.* **1980**, *40*, 213.

(2) Alagia, M.; Balucani, N.; Casavecchia, P.; Stranges, D.; Volpi, G. G. *J. Chem. Phys.* **1993**, *98*, 8341.

(3) Alagia, M.; Balucani, N.; Casavecchia, P.; Stranges, D.; Volpi, G. G.; Clary, D. C.; Kliesch, A.; Werner, H. *Chem. Phys.* **1996**, *207*, 389.

(4) Rochford, J. J.; Powell, L. J.; Grice, R. *J. Phys. Chem.* **1995**, *99*, 15369.

(5) Boodaghians, R. B.; Hall, I. W.; Wayne, R.P. *J. Chem. Soc., Faraday Trans. 2* **1987**, *83*, 529.

(6) Loewenstein, L. M.; Anderson, J. G. *J. Phys. Chem.* **1984**, *88*, 6277.

(7) Jenkin, M. E.; Clemitshaw, K. C.; Cox, R.A. *J. Chem. Soc., Faraday Trans. 2* **1984**, *80*, 1633.

(8) Loewenstein, L.M.; Anderson, J. G. *J. Phys. Chem.* **1985**, *89*, 5371.

(9) Rochford, J. J.; Powell, L. J.; Grice, R. *J. Phys. Chem.* **1995**, *99*, 13647.

(10) Powell, L. J.; Wells, D. D.; Wang, J. J.; Smith, D. J.; Grice, R. *Mol. Phys*. **1996**, *87*, 865.

(11) Pollard, J. E. *Rev. Sci. Instrum.* **1992**, *63*, 1771.

(12) Nowikow, C. V.; Grice, R. *J. Phys. E.* **1979**, *12*, 515.

(13) Entemann, E. A.; Herschbach, D. R. *Discuss. Faraday Soc.* **1967**, *44*, 289.

(14) Rusic, B.; Berkowitz, J. *J. Chem. Phys.* **1994**, *101*, 7795.

(15) Huber, K. P.; Herzberg, G. *Constants for Diatomic Molecules*; Van Nostrand Reinhold: New York, 1979.

(16) Fisk, G. A.; McDonald, J. D.; Herschbach, D. R. *Discuss. Faraday Soc.* **1967**, *44*, 228.

(17) Pechukas, P.; Light, J. C.; Rankin, C. *J. Chem. Phys.* **1966**, *44*, 794.

(18) Lin, J.; Light, J. C. *J. Chem. Phys.* **1966**, *45*, 2545.

(19) Light, J. C. *Discuss. Faraday Soc.* **1967**, *44*, 14.

(20) Walker, N.; Tevault, D. E.; Smardzewski, R. R. *J. Chem. Phys.* **1978**, *69*, 564.

(21) Klaassen, J. J.; Lindner, J.; Leone, S. R. *J. Chem. Phys.* **1996**, *104*, 7403.

(22) Wang, J. J.; Smith, D. J.; Grice, R. *Chem. Phys.* **1996**, *207*, 203.

(23) Herschbach, D. R. *Proc. Conf. Potential Energy Surfaces Chem.* **1970**, 44.

(24) Loewenstein, L. M.; Anderson, J. G. *J. Phys. Chem.* **1987**, *91*, 2993.

(25) White, R. W. P.; Smith, D. J.; Grice, R. *J. Phys. Chem.* **1993**, *97*, 2123.